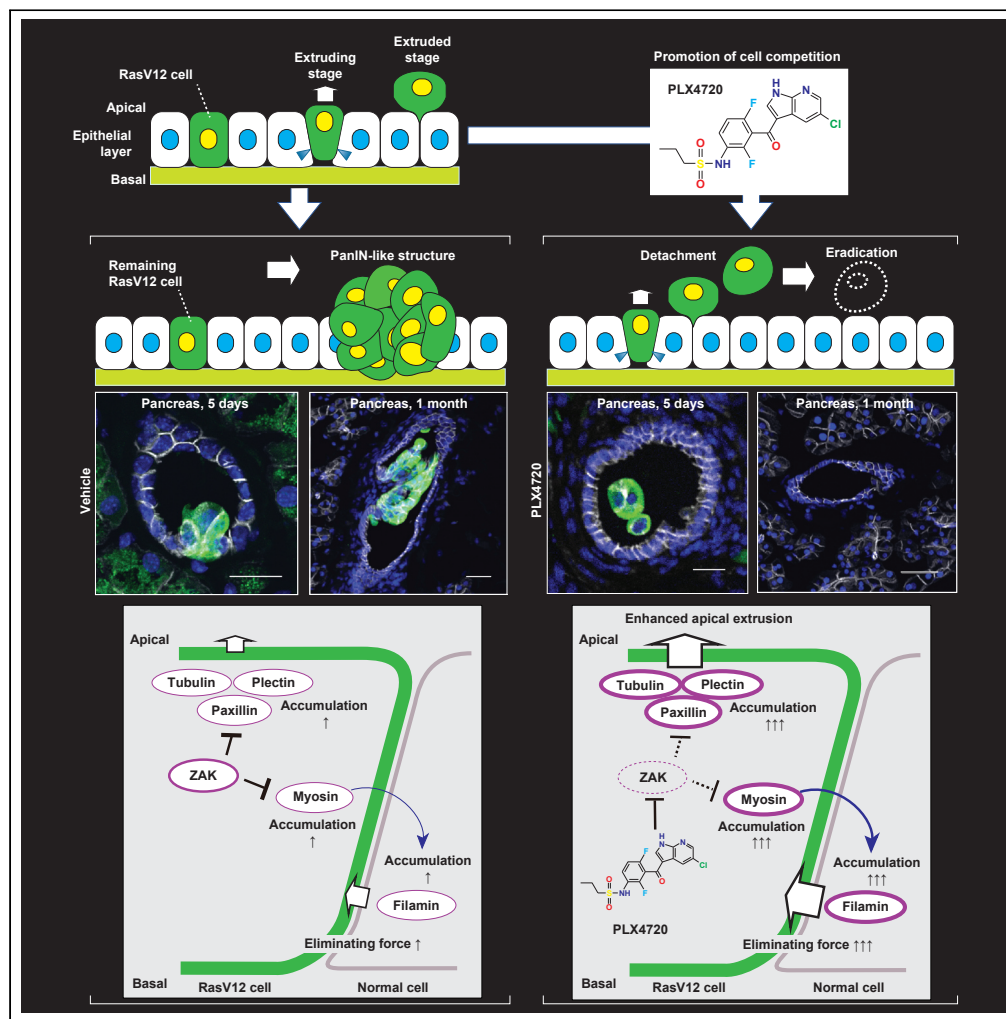# iScience

Article

ZAK Inhibitor PLX4720 Promotes Extrusion of Transformed Cells via Cell Competition

Takeshi Maruyama, Ayana Sasaki, Sayuri Iijima, ..., Susumu Ishikawa, Tomoko Morita, Yasuyuki Fujita

tmaru@aoni.waseda.jp (T.M.)
fujita@monc.med.kyoto-u.ac.jp (Y.F.)

HIGHLIGHTS

A cell competition-based high-throughput screen identifies chemical enhancers

PLX4720 enhances the apical elimination of RasV12 cells via ZAK inhibition

ZAK negatively modulates cell competition regulators

PLX4720 treatment promotes apical elimination of RasV12 cells *in vivo*

iScience

Article

ZAK Inhibitor PLX4720 Promotes Extrusion of Transformed Cells via Cell Competition

Takeshi Maruyama,[1,2,7,*] Ayana Sasaki,[1] Sayuri Iijima,[1] Shiyu Ayukawa,[3] Nobuhito Goda,[3] Keisuke Tazuru,[4] Norikazu Hashimoto,[4] Takashi Hayashi,[5] Kei Kozawa,[1] Nanami Sato,[1] Susumu Ishikawa,[1] Tomoko Morita,[1] and Yasuyuki Fujita[1,6,*]

SUMMARY

Previous studies have revealed that, at the initial step of carcinogenesis, transformed cells are often eliminated from epithelia via cell competition with the surrounding normal cells. In this study, we performed cell competition-based high-throughput screening for chemical compounds using cultured epithelial cells and confocal microscopy. PLX4720 was identified as a hit compound that promoted apical extrusion of RasV12-transformed cells surrounded by normal epithelial cells. Knockdown/knockout of ZAK, a target of PLX4720, substantially enhanced the apical elimination of RasV12 cells *in vitro* and *in vivo*. ZAK negatively modulated the accumulation or activation of multiple cell competition regulators. Moreover, PLX4720 treatment promoted apical elimination of RasV12-transformed cells *in vivo* and suppressed the formation of potentially precancerous tumors. This is the first report demonstrating that a cell competition-promoting chemical drug facilitates apical elimination of transformed cells *in vivo*, providing a new dimension in cancer preventive medicine.

INTRODUCTION

Despite extensive efforts in chemotherapeutic research, cancers are often resistant to chemical drugs. In addition, certain types of malignant tumors such as lung and pancreatic cancers are incurable even in the early stage detection (Jemal et al., 2006; Siegel et al., 2018). Recent studies using next-generation sequencing technology have revealed that, in our body, there are a number of abnormal lesions; although they apparently look normal, they comprise focally accumulated transformed cells that harbor just one or two oncogenic mutations (Martincorena et al., 2015, 2018). Hence, to overcome cancer, an alternative strategy would be a preventive cure: prophylactically eradicating such potentially pre-cancerous lesions.

Our recent studies have demonstrated that, at the initial stage of carcinogenesis, normal and transformed epithelial cells often compete with each other for survival: a phenomenon called cell competition (Maruyama and Fujita, 2017). For instance, when oncoprotein Ras- or Src-transformed cells are surrounded by normal epithelial cells, the transformed cells are extruded from the apical surface of the normal epithelial monolayer (Hogan et al., 2009; Kajita et al., 2010). These apically extruded transformed cells will eventually be eliminated from epithelial tissues and expelled outside the body (Kon et al., 2017; Sasaki et al., 2018), implying that this is a cancer preventive mechanism. During this cell competition process, normal epithelial cells first recognize the presence of neighboring transformed cells (Hogan et al., 2009). Normal cells then accumulate the cytoskeletal protein Filamin at the boundary with transformed cells, thereby generating physical forces and actively eliminating transformed cells from epithelia: a mechanism called epithelial defense against cancer (EDAC) (Kajita et al., 2014). On the other hand, the surrounded transformed cells also react to normal cells and accumulate a set of cytoskeletal components (Kadeer et al., 2017; Kasai et al., 2018; Ohoka et al., 2015; Saitoh et al., 2017). For example, Paxillin, Plectin, and Tubulin form a complex and accumulate at the apical side of transformed cells (Kadeer et al., 2017; Kasai et al., 2018). These three proteins mutually influence their non-cell-autonomous accumulation, which also plays a crucial role in apical extrusion of RasV12-transformed cells.

To identify chemical compounds that promote cell competition between normal and transformed cells, we have established a high-throughput screening platform based on epifluorescent microscopy and identified

Rebeccamycin as one of the hit compounds (Yamauchi et al., 2015). Rebeccamycin and its derivatives promote apical extrusion of transformed cells *in vitro*. However, these chemical compounds could not be applied to *in vivo* analyses because of their high cytotoxicity. In this study, we have newly established a confocal microscopy-based screening system and identified several chemical compounds that promote apical elimination of RasV12-transformed cells from epithelia *in vitro* and *in vivo*. This study will elicit future interest to establish cancer-preventive therapy by targeting cell competition.

RESULTS

PLX4720 and Its Derivatives Promote Apical Elimination of RasV12-Transformed Cells

To identify chemical compounds that promote apical extrusion of RasV12-transformed cells, we have optimized the previously established screening system (Yamauchi et al., 2015) by employing a confocal microscopy-based high-throughput platform (Figure 1A). First, normal MDCK cells and MDCK-pTR GFP-RasV12 cells were mixed at a ratio of 10:1 and cultured in a collagen-coated 96-well plate until they formed an epithelial monolayer. Then, the cells were incubated for 16 h with a small chemical compound, together with tetracycline to induce expression of GFP-RasV12. In this study, we used a chemical compound library consisting of various kinase inhibitors. Finally, apically extruded GFP-RasV12 cells were captured by confocal microscopic analyses (Figure S1A). After the primary screening, we obtained PLX4720 as a hit compound (Figure S1B). PLX4720 substantially enhanced apical extrusion of RasV12 cells that were surrounded by normal cells (Figure S1B), but not increased apical elimination of RasV12 cells that were cultured alone (Figure S1C). In addition, PLX4720 promoted apical extrusion in a dose-dependent manner (Figure 1B). Previous reports have demonstrated that PLX4720 strongly inhibits the activity of both ZAK and the active mutant of Raf (BRAF-V600E) but shows a much weaker inhibitory effect on wild-type Raf (Table S1) (Fabian et al., 2005; Karaman et al., 2008; Vin et al., 2013). ZAK, also called MLTK (MLK-like mitogen-activated protein triple kinase), is a member of the serine-threonine kinase MAPKKK family and is involved in osmotic stress response (Gotoh et al., 2001), but its role in cell competition has not been studied yet. We then found that other structurally related, ZAK-inhibiting compounds Vemurafenib and Dabrafenib significantly enhanced apical elimination of MDCK-pTR GFP-RasV12 cells from a monolayer of normal MDCK cells (Figures 1C–1E and Table S1). MDCK cells do not harbor V600E mutations in the *BRAF* gene locus. In addition, an inhibitor of the BRAF downstream kinase MEK suppresses apical elimination of RasV12-transformed cells (Hogan et al., 2009). Thus, it is plausible that the effect of these compounds on apical extrusion of RasV12 cells is attributed to inhibition of ZAK, rather than that of Raf.

ZAK Is a Negative Regulator for Apical Extrusion of RasV12-Transformed Cells

These three compounds share a similar chemical structure (Figure 1C) that is, at least partly, involved in the occupancy of the ATP pocket of the ZAK kinase domain (Mathea et al., 2016). Therefore, we tested a structurally distinct ZAK inhibitor Sorafenib (Figure 2A) and found that addition of Sorafenib also substantially promoted apical extrusion of RasV12 cells (Figure 2B) (Vin et al., 2014). These results suggest that ZAK plays a negative role in the elimination of transformed cells. To validate a functional role of ZAK, we depleted ZAK either in normal or RasV12-transformed cells using CRISPR-Cas9 technology and successfully generated homozygous ZAK-knockout cells, which possess 2 base-depletion (ZAK-KO1) or 17 base-insertion (ZAK-KO2). ZAK knockout in normal cells did not affect the frequency of extrusion (Figures 2C and S2A). In contrast, ZAK knockout in RasV12-transformed cells significantly enhanced apical extrusion (Figures 2D and S2B). Exogenous expression of wild-type (WT) ZAK rescued the phenotype but that of kinase-negative ZAK did not (Figures 2DI, S2B, and S2C), suggesting a crucial role of ZAK kinase activity. Accordingly, apical extrusion of ZAK-knockout RasV12 cells was not affected by PLX4720 (Figures 2E and S2D). These results indicate that the kinase activity of ZAK in RasV12 cells negatively regulates apical extrusion. To further investigate the prevalent role of ZAK in elimination of transformed cells, we examine the effect of ZAK knockdown *in vivo* using the mouse cell competition model system (Villin-CreERT2; LSL-RasV12-IRES-eGFP) (Figure 2F) (Kon et al., 2017). To induce ZAK knockdown *in vivo*, we used the iGT (intestine-specific gene transfer) system by which short interfering RNA (siRNA) can be introduced into mouse intestinal epithelia using electroporation (Imajo et al., 2015). First, we conducted *in vivo* electroporation with control- or ZAK-siRNA, and then a low dose of tamoxifen was administered to induce the expression of the RasV12 protein in a mosaic manner within intestinal epithelia (Figure 2G) (Kon et al., 2017). The introduction of ZAK-siRNA#1 diminished the expression of ZAK (Figures S2E and S2F) and significantly promoted apical elimination of RasV12-expressing cells from the epithelium (Figures 2H and 2I). Collectively, these results demonstrate that ZAK is a crucial negative regulator for apical extrusion of RasV12-transformed cells from epithelia *in vitro* and *in vivo*.
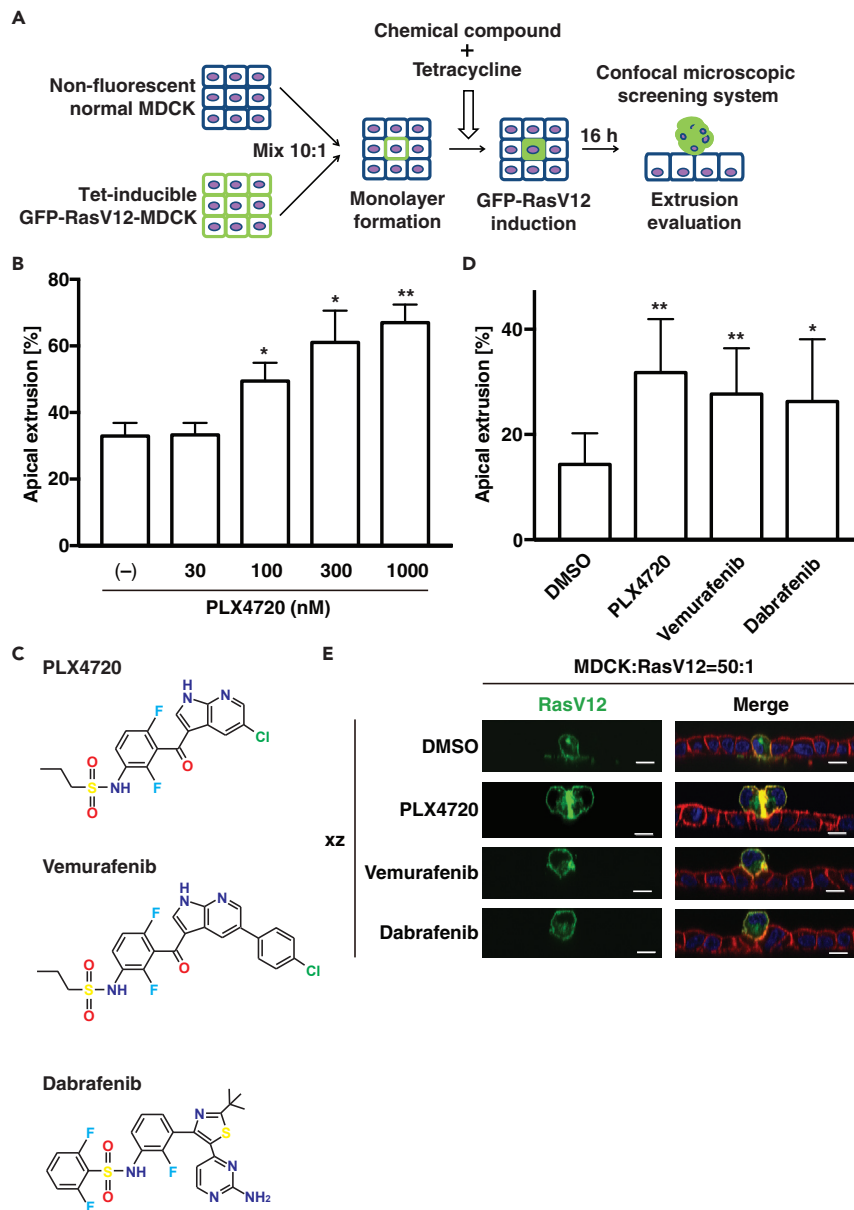
Figure 1. Cell Competition-Based High-Throughput Screening for Chemical Compounds Using Confocal Microscopy

(A) A scheme of cell competition-based screening.

(B) The dose-dependent effect of PLX4720 on apical extrusion of RasV12-transformed cells.

(C) Chemical structure of PLX4720 and its derivative compounds.

(D and E) The effect of PLX4720 and its derivative compounds (1 μM) on apical extrusion of RasV12-transformed cells.

(B, D, and E) MDCK-pTR GFP-RasV12 cells were mixed with normal MDCK cells on collagen gels. Cells were cultured with the indicated chemical compounds and fixed after 16 h incubation with tetracycline and stained with phalloidin (red) and Hoechst (blue). (B and D) Quantification of apical extrusion of RasV12 cells. n ≧ 100 cells for each experimental condition. Data are mean ± SD from three independent experiments. *p < 0.05, **p < 0.01 (Student's t tests). (E) Representative XZ images of normal and RasV12 cells. Scale bars: 10 μm.

ZAK Negatively Modulates Cell Competition Regulators

At the interface between normal and RasV12-transformed cells, various non-cell autonomous changes occur in both normal and transformed cells. For instance, in RasV12-transformed cells, the adaptor protein Paxillin is accumulated, and the activity of Myosin-II is elevated (Hogan et al., 2009; Kasai et al., 2018). In
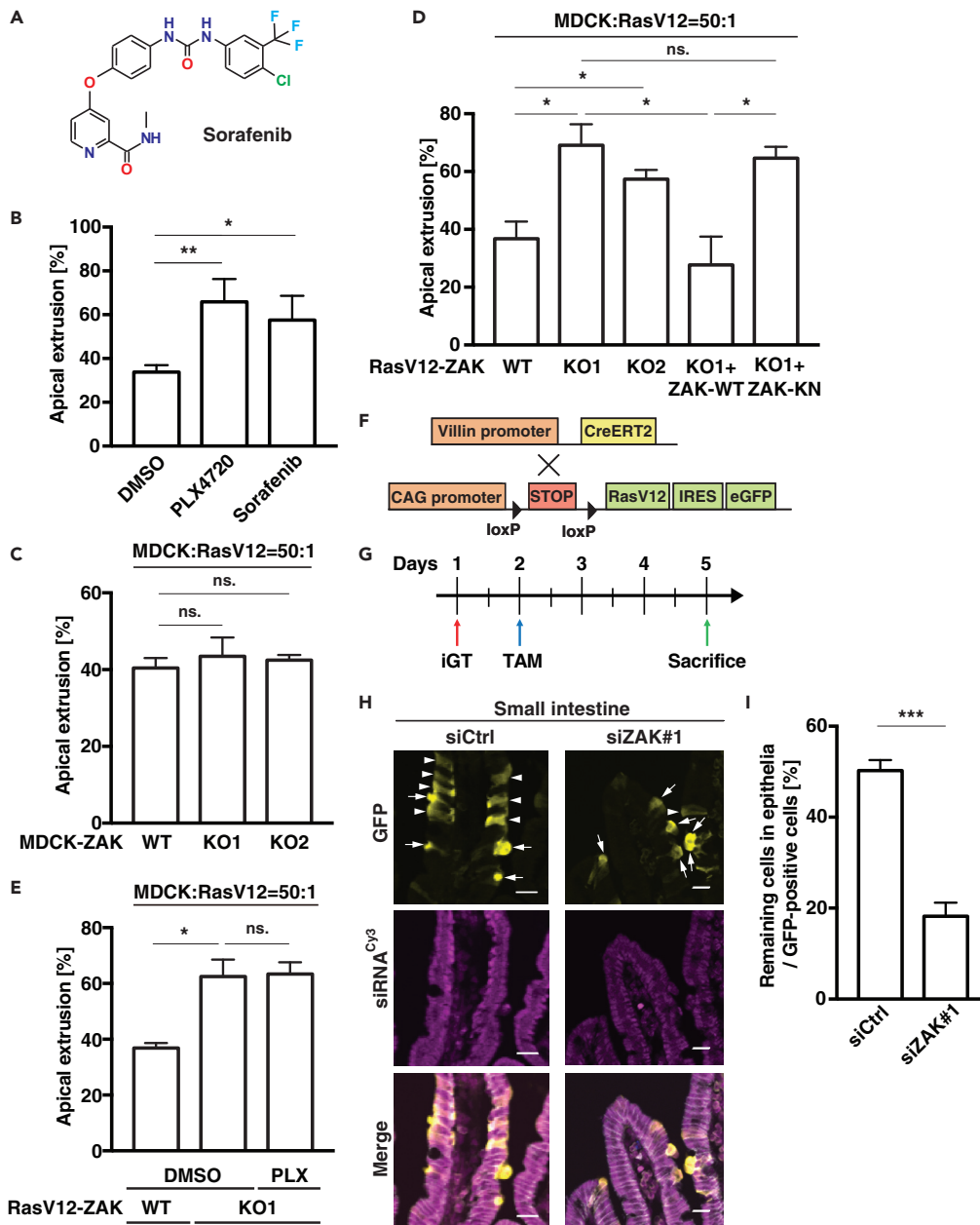
Figure 2. ZAK Negatively Regulates Apical Extrusion of RasV12-Transformed Cells *In Vitro* and *In Vivo*

(A) The chemical structure of Sorafenib.

(B) Sorafenib, another ZAK inhibitor, promotes apical extrusion of RasV12-transformed cells. MDCK-pTR GFP-RasV12 cells were mixed with normal MDCK cells on collagen gels. The cells were fixed after 24 h incubation with tetracycline together with DMSO, PLX4720, or Sorafenib (1 μM).

(C) Knockout of ZAK in normal cells does not affect the efficiency of apical extrusion. MDCK-pTR GFP-RasV12 cells were mixed with normal MDCK ZAK-WT or -KO cells on collagen gels. The cells were fixed after 24 h incubation with tetracycline, and apical extrusion was quantified.

(D) Knockout of ZAK in RasV12-transformed cells promotes apical extrusion. MDCK-pTR GFP-RasV12 ZAK-wild-type (WT), ZAK-knockout (KO), ZAK-KO + HA-ZAK-WT, or ZAK-KO + HA-ZAK-kinase-negative (KN) cells were mixed with normal MDCK cells on collagen gels. The cells were fixed after 24 h incubation with tetracycline, and apical extrusion was quantified. (B–D) n ≧ 100 cells for each experimental condition. Data are mean ± SD from three independent experiments. *p < 0.05, **p < 0.01, ns.: not significant (Student's t tests).

(E) PLX4720 does not enhance the extrusion efficiency of ZAK-knockout RasV12 cells. MDCK-pTR GFP-RasV12 ZAK-wild-type (WT) or ZAK-KO cells were mixed with normal MDCK cells on collagen gels. The cells were fixed after 24 h incubation

Figure 2. *Continued*

with PLX4720 and tetracycline, and the frequency of apical extrusion was quantified. n≧100 cells for each experimental condition. Data are mean ± SD from three independent experiments. *p < 0.05, ns.: not significant (Student's t tests).

(F)Strategy for the establishment of the cell competition mouse model using an intestine-specific Villin-CreERT2 system.

(G) Experimental design for short-term tamoxifen (TAM) administration on the small intestine after siRNA introduction by electroporation-based intestinal gene transfer (iGT).

(H and I) Knockdown of ZAK promotes apical extrusion within intestinal epithelia. (H) Immunofluorescence images of RasV12-transformed cells in the epithelium of the small intestine. The intestine tissue samples with Control-siRNA (siCtrl) or ZAK-siRNA#1 (siZAK#1) were stained with anti-GFP (yellow) and anti-E-cadherin (gray) antibodies and Cy3 (magenta). Scale bars: 20 μm. (I) Quantification of apical extrusion of RasV12 cells in the small intestine. siCtrl 345 transformed cells from three mice; siZAK#1 280 transformed cells from three mice. ***p < 0.005 (chi-square test).

addition, in normal cells, the cytoskeletal protein Filamin is accumulated at the boundary with transformed cells (Kajita et al., 2014). Importantly, accumulation or activation of these molecules, in concert, positively regulate apical extrusion of transformed cells. We thus investigated the effect of ZAK knockout in Ras-transformed cells on these processes. We observed that ZAK knockout significantly promoted the accumulation of Paxillin (Figures 3A and 3B). In addition, the level of phospho-Myosin light chain (phospho-MLC), which reflects the activity of Myosin-II, increased in the ZAK-knockout transformed cells (Figures 3C and 3D). Moreover, ZAK knockout promoted the accumulation of Filamin in normal cells at the interface with Ras-transformed cells (Figures 3E and 3F). Consistently, addition of PLX4720 also facilitated the phosphorylation of MLC and the accumulation of Filamin (Figure S3). These findings suggest that ZAK negatively modulates the cell competition regulators, thereby suppressing apical extrusion of transformed cells.

PLX4720 Treatment Promotes Apical Elimination of RasV12-Transformed Cells *In Vivo*

Finally, using the cell competition mouse model, we examined the effect of PLX4720 on elimination of transformed cells *in vivo*. The oncogenic mutation in the *Ras* gene occurs at the initial stage of pancreatic cancer and is involved in the formation of pancreatic intraepithelial neoplasia (PanIN), precancerous lesions in the pancreas (Bardeesy and DePinho, 2002; Morris et al., 2010). Thus, we evaluated the extrusion efficiency within the epithelia of pancreatic ducts. To monitor the fate of newly emerging RasV12-transformed cells in ductal epithelia of the pancreas, we crossed LSL-RasV12-IRES-EGFP mice with cytokeratin 19 (CK19) (epithelial-specific marker)-Cre-ERT2 mice (Figure 4A). According to the remaining level of PLX4720 in the pancreas after oral administration (Figure S4), 300 mg/kg PLX4720 was administered twice per day (Figure 4B). As previously reported (Sasaki et al., 2018), when PLX4720 was not administered, GFP-positive RasV12-expressing cells often remained within epithelia (Figures 4C and 4D). In contrast, after 5 days of PLX4720 administration, most of RasV12-expressing cells were apically detached into the ductal lumen or absent within the pancreatic ducts (Figures 4C and 4D). As a control, YFP-expressing cells just remained in the epithelia, and PLX4720 did not affect the rate of YFP-positive cells in the pancreatic ducts (Figures 4E–4G). After 1 month of tamoxifen treatment, some remaining RasV12 cells proliferated and formed a PanIN-like tumorous structure (Figures 4H and 4I). But, PLX4720 administration profoundly decreased the number of remaining RasV12-expressing cells (Figures 4I and 4J). Collectively, these results demonstrate that PLX4720 treatment promotes apical elimination of RasV12-transformed cells *in vivo* and suppresses the formation of potentially precancerous tumors.

DISCUSSION

Pancreatic cancer is one of the major causes of cancer-associated mortality, and the prognosis has remained seriously poor. The most common mutations are *KRAS, TP53,* and *SMAD4*, none of which are, however, currently druggable targets (Kleeff et al., 2016). Therefore, a novel approach for early diagnosis and preventive treatment at the curable stage would be desired. In this study, we have identified chemical compounds that enhance apical elimination of RasV12-transformed cells, a cancer preventive process. Especially, PLX4720 suppresses the formation of pre-cancerous tumors within the pancreatic ducts. The number of the apically delaminated RasV12 cells decreases as time goes by after PLX4720 administration, suggesting that the apically detached cells would undergo anoikis or be eradicated outside the body. Thus, PLX4720 treatment would contribute to a decreased risk of carcinogenesis. This is the first report demonstrating that a cell competition-promoting chemical drug facilitates apical elimination of transformed cells *in vivo*.

Previous studies have demonstrated that PLX4720 strongly inhibits the activity of both ZAK and the active mutant of Raf (BRAF-V600E) but not that of wild-type Raf (Fabian et al., 2005; Karaman et al., 2008; Vin et al., 2013). Instead, PLX4720 can cause paradoxical activation of wild-type Raf (Hatzivassiliou et al., 2010;
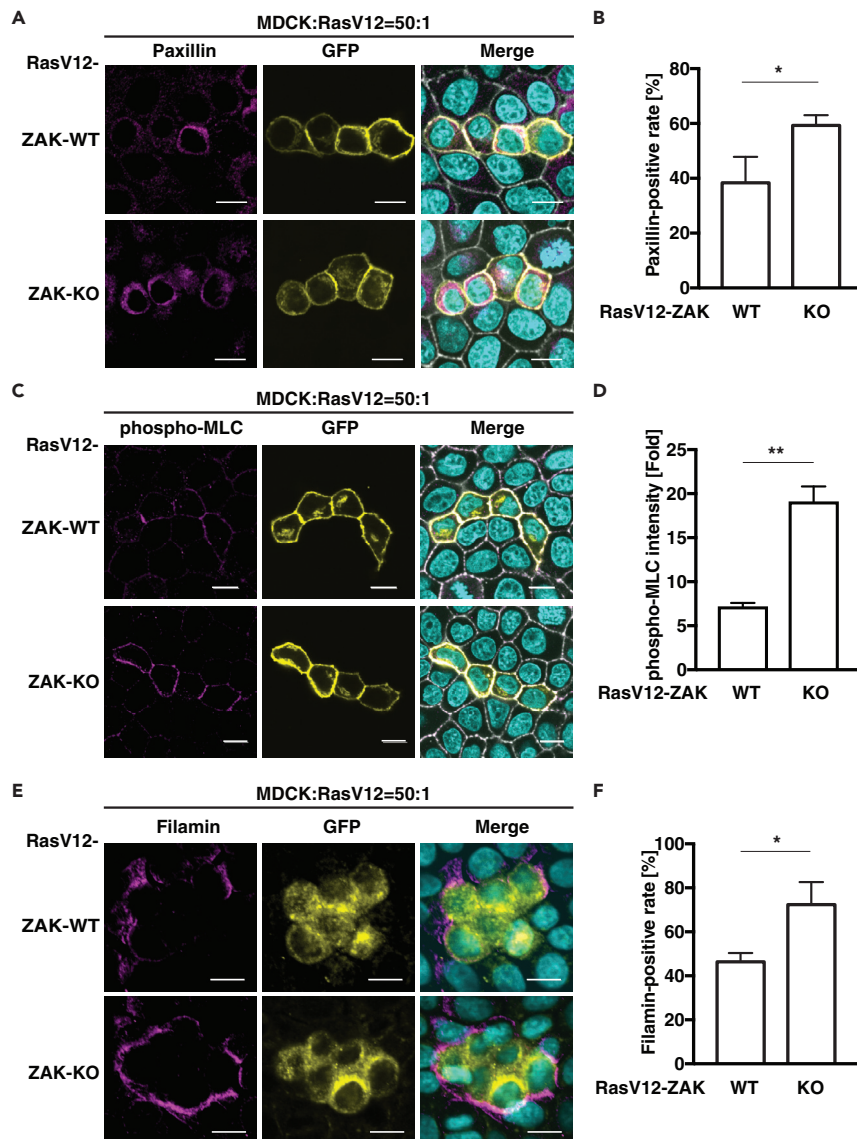
Figure 3. ZAK Negatively Modulates Cell Competition Regulators

(A–D) ZAK-KO promotes accumulation of Paxillin (A and B) or phosphorylation light chain of Myosin-II (phospho-MLC) in RasV12 cells surrounded by normal cells. MDCK-pTR GFP-RasV12 ZAK-wild-type (WT) or ZAK-knockout (KO) cells were mixed with normal MDCK cells on collagen gels. The cells were fixed after 16 h incubation with tetracycline and stained with anti-Paxillin (A and B) or phospho-MLC (C and D) antibody (magenta), Alexa-Fluor-647-phalloidin (gray), and Hoechst (cyan). The positive rate of Paxillin staining was quantified. For phospho-MLC quantification, the fluorescence intensity at the boundary between respective RasV12 cells and normal cells were expressed as fold change relative to the average fluorescence intensity between the surrounding normal cells. $n \geqq 100$ cells for each experimental condition. Data are mean $\pm$ SD from three independent experiments. $*p < 0.05$, $**p < 0.01$ (Student's t tests).

(E and F) ZAK-KO in RasV12 cells promotes accumulation of Filamin in the neighboring normal cells. MDCK-pTR GFP-RasV12 wild-type (WT) or ZAK-knockout (KO) cells were mixed with normal MDCK cells on collagen gels. The cells were fixed after 16 h incubation with tetracycline and stained with anti-Filamin antibody (magenta) and Hoechst (cyan) (E). The positive rate of Filamin accumulation in surrounding normal cells was quantified (F). $n \geqq 100$ cells for each experimental condition. Data are mean $\pm$ SD from three independent experiments. $*p < 0.05$ (Student's t tests).

Poulikakos et al., 2010). Indeed, the slight activation of ERK is observed upon PLX4720 treatment in MDCK cells (data not shown), implying that PLX4720 induces attenuation of ZAK activity as well as ERK activation, which might promote apical elimination of transformed cells in an orchestrated fashion. Additionally, the involvement of other kinases, the activity of which could be potentially inhibited by ZAK inhibitors, cannot
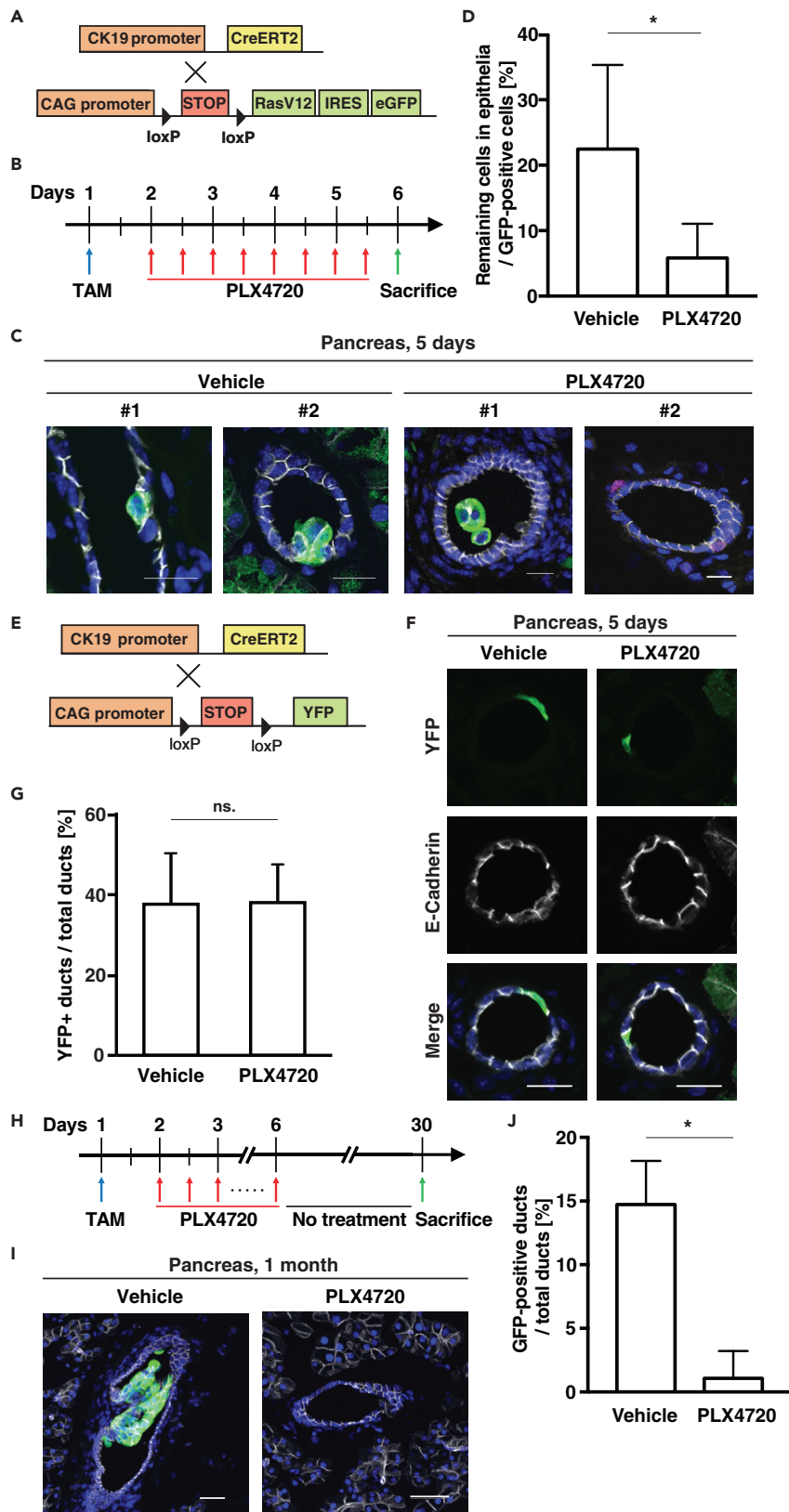
Figure 4. PLX4720 Treatment Suppresses Apical Extrusion of RasV12-Transformed Cells from Pancreatic Ductal Epithelia

(A and E) The cell competition mouse model using a CK19-CreERT2 system and control YFP mouse.

(B and H) Experimental designs for short-term (B) or long-term (H) Tamoxifen (TAM)-PLX4720 administration.

(C and I) Immunofluorescence images of RasV12-transformed cells in the epithelium of the pancreatic ducts upon short-term (C) or long-term (I) vehicle or PLX4720 treatment. The tissue samples were stained with anti-GFP (green) and anti-E-cadherin (gray) antibodies and Hoechst (blue). Scale bars: 20 μm.

(D) Quantification of apical extrusion of RasV12 cells for (C). Vehicle 86 cells from four mice; PLX4720 153 cells from five mice. *p < 0.05 (chi-square test).

(F) Immunofluorescence images of YFP-expressing cells in the epithelium of the pancreatic ducts with or without PLX4720 treatment after low-dose TAM administration. The tissue samples were stained with anti-GFP (green) and anti-E-cadherin (gray) antibodies and Hoechst (blue). Scale bars: 20 μm.

(G) Quantification of remaining YFP-expressing cells within epithelia for (F). Vehicle 196 cells from four mice; PLX4720 204 cells from four mice. Data are mean ± SD from four independent mice. ns.: not significant (chi-square test).

(I and J) (J) Quantification of apical extrusion of RasV12 cells for (I). Vehicle 584 ducts from five mice; PLX4720 500 ducts from four mice. *p < 0.05 (chi-square test).

be ruled out (Karaman et al., 2008; Vin et al., 2013). However, a structurally distinct ZAK inhibitor Sorafenib or ZAK knockout enhances apical extrusion, indicating that suppression of ZAK alone is sufficient to regulate this process. ZAK is a family member of MAPKKK (Gotoh et al., 2001), but its function remains enigmatic. We demonstrate that ZAK is a novel key regulator for cell competition between normal and RasV12-transformed cells. ZAK activity in RasV12 cells plays a negative role in their apical extrusion by modulating the activity or localization of downstream cell competition regulators: Paxillin and Myosin-II in RasV12 cells and filamin in normal cells. However, it remains to be uncovered what are the direct substrate proteins of ZAK in this process. ZAK is reported to upregulate the activity of ERK, JNK, and p38 upon various stimuli such as inflammation and osmotic stress (Gotoh et al., 2001; Wong et al., 2013; Yang et al., 2010). Further studies would be required to understand more detailed molecular mechanisms of this ZAK-regulated cell extrusion.

A previous study using a cell competition mouse model has revealed that obesity and obesity-induced chronic inflammation diminish apical elimination of RasV12-transformed cells in the small intestine and pancreas (Sasaki et al., 2018). These environmental conditions affect apical elimination of transformed cells, leading to the formation of precancerous lesions. In addition, inflammation can induce ZAK-mediated activation of JNK and p38 (Wong et al., 2013). Given that the inflammation suppresses apical extrusion (Sasaki et al., 2018) and activates the ZAK-JNK/p38 pathway, it is plausible that obesity-induced inflammation suppresses elimination of transformed cells, at least partly, through modulation of the ZAK-JNK/p38 pathway. It will be tested whether the PLX4720 treatment can promote the extrusion of the remaining RasV12-transformed cells under these environmental conditions.

A recent study demonstrates that cell competition can occur during the process of carcinogenesis in human (Madan et al., 2019). Moreover, several lines of studies have revealed that there are a number of focally colonized transformed cells in our bodies and that these precancerous lesions progressively accumulate with age. Hence, this study would shed light on those clinically unexplored lesions and provide a new dimension in cancer preventive medicine. Further elucidation of cell competition mechanisms would pave a way to cancer prophylactic treatment.

Limitations of the Study

Our study has some limitations. First, it remains to be uncovered what the direct substrate proteins of ZAK are. Second, to promote accumulation of Myosin-II, the substrate of ZAK should regulate Myosin-II accumulation. In this case, the substrate needs to be identified. In addition, it is also a possibility that direct regulation of Myosin-II by ZAK contributes to promoting stiffness of RasV12 cells by accumulation of Myosin-II at the boundary. Last, it is required that PanIN-like structure is related to tumorigenesis and the PLX is further analyzed in-depth using tumor growth in the xenograft model.

Resource Availability

Lead Contact

Further information and requests for resources and reagents should be directed to and will be fulfilled by the Lead Contact, Takeshi Maruyama (tmaru@aoni.waseda.jp).

Materials Availability

Materials generated in this study are available from the corresponding author on requests.

Data and Code Availability

The original dataset generated during this study will be publicly available.

Data: https://doi.org/10.17632/m296vz4d9d.1.

METHODS

All methods can be found in the accompanying Transparent Methods supplemental file.

SUPPLEMENTAL INFORMATION

Supplemental Information can be found online at https://doi.org/10.1016/j.isci.2020.101327.

AUTHOR CONTRIBUTIONS

T. Maruyama designed experiments and generated most of the data. A.S., S. Iijima, S.A., K.T., T.H., and T. Morita performed experiments. K.T. and N.H. performed the primary chemical compound screening. N.G., T.H., and N.H. assisted with data analysis. K.K., N.S., and S. Ishikawa assisted with experiments. T.H. performed the mass-spectrometric analysis for PLX4720 remaining in tissues. Y.F. conceived and designed the study. The manuscript was written by T. Maruyama and Y.F. with assistance from the other authors.

DECLARATION OF INTERESTS

The authors declare no competing of interest.

REFERENCES

Bardeesy, N., and DePinho, R.A. (2002). Pancreatic cancer biology and genetics. Nat. Rev. Cancer *2*, 897–909.

Fabian, M.A., Biggs, W.H., 3rd, Treiber, D.K., Atteridge, C.E., Azimioara, M.D., Benedetti, M.G., Carter, T.A., Ciceri, P., Edeen, P.T., Floyd, M., et al. (2005). A small molecule-kinase interaction map for clinical kinase inhibitors. Nat. Biotechnol. *23*, 329–336.

Gotoh, I., Adachi, M., and Nishida, E. (2001). Identification and characterization of a novel MAP kinase kinase kinase. MLTK. J. Biol. Chem. *276*, 4276–4286.

Hatzivassiliou, G., Song, K., Yen, I., Brandhuber, B.J., Anderson, D.J., Alvarado, R., Ludlam, M.J., Stokoe, D., Gloor, S.L., Vigers, G., et al. (2010). RAF inhibitors prime wild-type RAF to activate the MAPK pathway and enhance growth. Nature *464*, 431–435.

Hogan, C., Dupre-Crochet, S., Norman, M., Kajita, M., Zimmermann, C., Pelling, A.E., Piddini, E., Baena-Lopez, L.A., Vincent, J.P., Itoh, Y., et al. (2009). Characterization of the interface between normal and transformed epithelial cells. Nat. Cell Biol *11*, 460–467.

Imajo, M., Ebisuya, M., and Nishida, E. (2015). Dual role of YAP and TAZ in renewal of the intestinal epithelium. Nat. Cell Biol *17*, 7–19.

Jemal, A., Siegel, R., Ward, E., Murray, T., Xu, J., Smigal, C., and Thun, M.J. (2006). Cancer statistics, 2006. CA Cancer J. Clin. *56*, 106–130.

Kadeer, A., Maruyama, T., Kajita, M., Morita, T., Sasaki, A., Ohoka, A., Ishikawa, S., Ikegawa, M., Shimada, T., and Fujita, Y. (2017). Plectin is a novel

regulator for apical extrusion of RasV12-transformed cells. Sci. Rep. 7, 44328.

Kajita, M., Hogan, C., Harris, A.R., Dupre-Crochet, S., Itasaki, N., Kawakami, K., Charras, G., Tada, M., and Fujita, Y. (2010). Interaction with surrounding normal epithelial cells influences signalling pathways and behaviour of Src-transformed cells. J. Cell Sci 123, 171–180.

Kajita, M., Sugimura, K., Ohoka, A., Burden, J., Suganuma, H., Ikegawa, M., Shimada, T., Kitamura, T., Shindoh, M., Ishikawa, S., et al. (2014). Filamin acts as a key regulator in epithelial defence against transformed cells. Nat. Commun. 5, 4428.

Karaman, M.W., Herrgard, S., Treiber, D.K., Gallant, P., Atteridge, C.E., Campbell, B.T., Chan, K.W., Ciceri, P., Davis, M.I., Edeen, P.T., et al. (2008). A quantitative analysis of kinase inhibitor selectivity. Nat. Biotechnol. 26, 127–132.

Kasai, N., Kadeer, A., Kajita, M., Saitoh, S., Ishikawa, S., Maruyama, T., and Fujita, Y. (2018). The paxillin-plectin-EPLIN complex promotes apical elimination of RasV12-transformed cells by modulating HDAC6-regulated tubulin acetylation. Sci. Rep. 8, 2097.

Kleeff, J., Korc, M., Apte, M., La Vecchia, C., Johnson, C.D., Biankin, A.V., Neale, R.E., Tempero, M., Tuveson, D.A., Hruban, R.H., et al. (2016). Pancreatic cancer. Nat. Rev. Dis. Primers 2, 16022.

Kon, S., Ishibashi, K., Katoh, H., Kitamoto, S., Shirai, T., Tanaka, S., Kajita, M., Ishikawa, S., Yamauchi, H., Yako, Y., et al. (2017). Cell competition with normal epithelial cells promotes apical extrusion of transformed cells through metabolic changes. Nat. Cell Biol 19, 530–541.

Madan, E., Pelham, C.J., Nagane, M., Parker, T.M., Canas-Marques, R., Fazio, K., Shaik, K., Yuan, Y., Henriques, V., Galzerano, A., et al. (2019). Flower isoforms promote competitive growth in cancer. Nature 572, 260–264.

Martincorena, I., Fowler, J.C., Wabik, A., Lawson, A.R.J., Abascal, F., Hall, M.W.J., Cagan, A., Murai, K., Mahbubani, K., Stratton, M.R., et al. (2018). Somatic mutant clones colonize the human esophagus with age. Science 362, 911–917.

Martincorena, I., Roshan, A., Gerstung, M., Ellis, P., Van Loo, P., McLaren, S., Wedge, D.C., Fullam, A., Alexandrov, L.B., Tubio, J.M., et al. (2015). Tumor evolution. High burden and pervasive positive selection of somatic mutations in normal human skin. Science 348, 880–886.

Maruyama, T., and Fujita, Y. (2017). Cell competition in mammals - novel homeostatic machinery for embryonic development and cancer prevention. Curr. Opin. Cell Biol 48, 106–112.

Mathea, S., Abdul Azeez, K.R., Salah, E., Tallant, C., Wolfreys, F., Konietzny, R., Fischer, R., Lou, H.J., Brennan, P.E., Schnapp, G., et al. (2016). Structure of the human protein kinase ZAK in complex with Vemurafenib. ACS Chem. Biol. 11, 1595–1602.

Morris, J.P.t., Wang, S.C., and Hebrok, M. (2010). KRAS, Hedgehog, Wnt and the twisted developmental biology of pancreatic ductal adenocarcinoma. Nat. Rev. Cancer 10, 683–695.

Ohoka, A., Kajita, M., Ikenouchi, J., Yako, Y., Kitamoto, S., Kon, S., Ikegawa, M., Shimada, T., Ishikawa, S., and Fujita, Y. (2015). EPLIN is a crucial regulator for extrusion of RasV12-transformed cells. J. Cell Sci 128, 781–789.

Poulikakos, P.I., Zhang, C., Bollag, G., Shokat, K.M., and Rosen, N. (2010). RAF inhibitors transactivate RAF dimers and ERK signalling in cells with wild-type BRAF. Nature 464, 427–430.

Saitoh, S., Maruyama, T., Yako, Y., Kajita, M., Fujioka, Y., Ohba, Y., Kasai, N., Sugama, N., Kon, S., Ishikawa, S., et al. (2017). Rab5-regulated endocytosis plays a crucial role in apical extrusion of transformed cells. Proc. Natl. Acad. Sci. U S A 114, E2327–E2336.

Sasaki, A., Nagatake, T., Egami, R., Gu, G., Takigawa, I., Ikeda, W., Nakatani, T., Kunisawa, J., and Fujita, Y. (2018). Obesity suppresses cell-competition-mediated apical elimination of RasV12-transformed cells from epithelial tissues. Cell Rep 23, 974–982.

Siegel, R.L., Miller, K.D., and Jemal, A. (2018). Cancer statistics, 2018. CA Cancer J. Clin. 68, 7–30.

Vin, H., Ching, G., Ojeda, S.S., Adelmann, C.H., Chitsazzadeh, V., Dwyer, D.W., Ma, H., Ehrenreiter, K., Baccarini, M., Ruggieri, R., et al. (2014). Sorafenib suppresses JNK-dependent apoptosis through inhibition of ZAK. Mol. Cancer Ther. 13, 221–229.

Vin, H., Ojeda, S.S., Ching, G., Leung, M.L., Chitsazzadeh, V., Dwyer, D.W., Adelmann, C.H., Restrepo, M., Richards, K.N., Stewart, L.R., et al. (2013). BRAF inhibitors suppress apoptosis through off-target inhibition of JNK signaling. Elife 2, e00969.

Wong, J., Smith, L.B., Magun, E.A., Engstrom, T., Kelley-Howard, K., Jandhyala, D.M., Thorpe, C.M., Magun, B.E., and Wood, L.J. (2013). Small molecule kinase inhibitors block the ZAK-dependent inflammatory effects of doxorubicin. Cancer Biol. Ther. 14, 56–63.

Yamauchi, H., Matsumaru, T., Morita, T., Ishikawa, S., Maenaka, K., Takigawa, I., Semba, K., Kon, S., and Fujita, Y. (2015). The cell competition-based high-throughput screening identifies small compounds that promote the elimination of RasV12-transformed cells from epithelia. Sci. Rep. 5, 15336.

Yang, J.J., Lee, Y.J., Hung, H.H., Tseng, W.P., Tu, C.C., Lee, H., and Wu, W.J. (2010). ZAK inhibits human lung cancer cell growth via ERK and JNK activation in an AP-1-dependent manner. Cancer Sci. 101, 1374–1381.

Supplemental Information

ZAK Inhibitor PLX4720 Promotes Extrusion

of Transformed Cells via Cell Competition

Takeshi Maruyama, Ayana Sasaki, Sayuri Iijima, Shiyu Ayukawa, Nobuhito Goda, Keisuke Tazuru, Norikazu Hashimoto, Takashi Hayashi, Kei Kozawa, Nanami Sato, Susumu Ishikawa, Tomoko Morita, and Yasuyuki Fujita
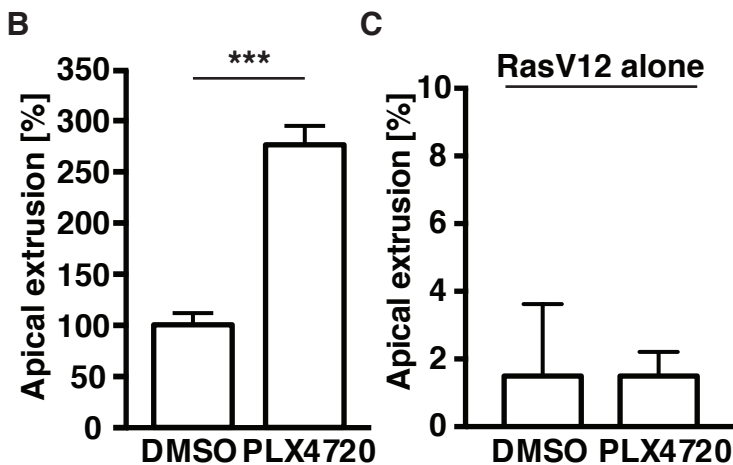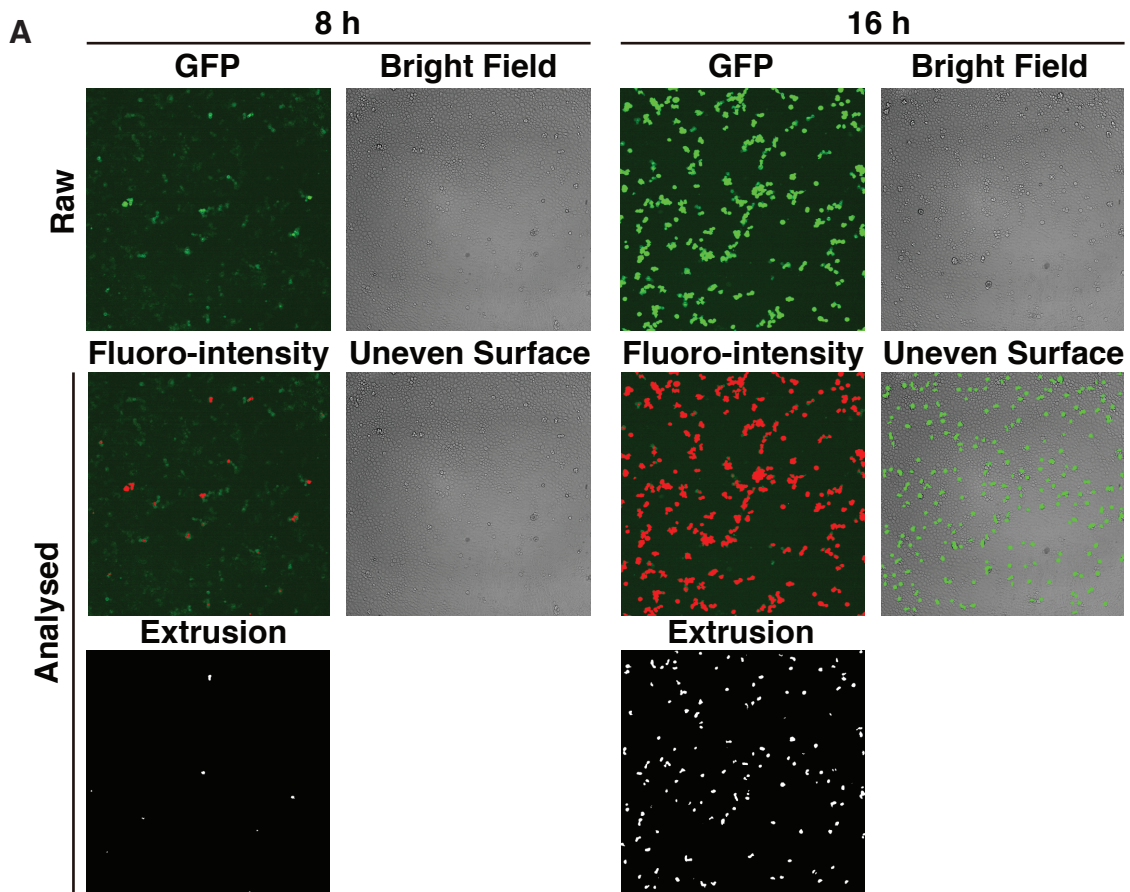
Figure S1. The establishment of a high-throughput screening platform using confocal microscopy, related to Figure 1 (A) MDCK cells were mixed with MDCK-pTR GFP-RasV12 cells and seeded into a collagen-coated 96-well plate. The mixed cells were incubated until a monolayer was formed. Then, the culture medium was exchanged for new medium containing 10 μg/ml tetracycline, followed by incubation for 16 h. Cells were fixed and stained with Hoechst 33342 and Alexa555-Phalloidin. The images of cells were captured using a confocal imaging analyzer, and GFP-fluorescent and Bright field images were acquired. The GFP-positive cells were selected by GFP intensities as shown in red in the panel 'Analysed-Fluoro-intensity'. The uneven surface area was independently analysed using a 65536-gradient step bright-field and shown as light green in the panel 'Analysed-Uneven Suface'. Double positive cells are extracted as white spots as shown in the panel 'Analysed-Extrusion' and defined as apically extruded RasV12 cells. (B) The validation assay showing the effect of 10 μM PLX4720 on apical extrusion of RasV12 cells. Data are mean ± SD from three independent experiments. ***P<0.005 (Student's *t*-tests). (C) PLX4720 did not affect the RasV12-transformed cells in the condition of RasV12 alone. Data are mean ± SD from three independent experiments.
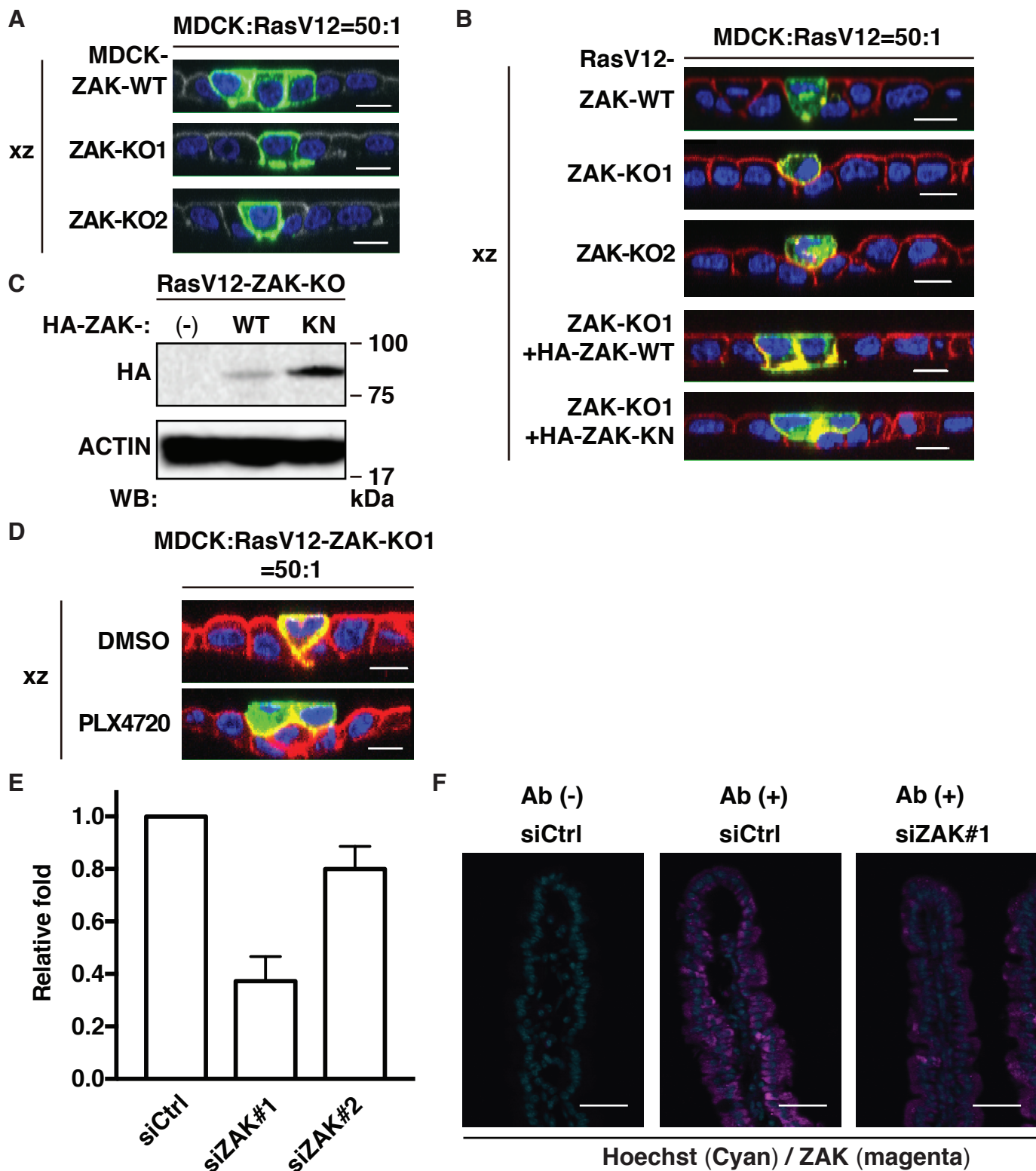
Figure S2. Supplementary figures for Figure 2
ZAK-knockout in RasV12-transformed cells promotes apical extrusion (A) Representative XZ images for Figure 2c. Phalloidin and Hoechst staining are shown in grey and blue, respectively. Scale bars: 10 μm. (B) MDCK-pTR GFP-RasV12 ZAK-wild-type (WT) cells or ZAK-KO cells constitutively expressing HA-ZAKα-WT or -KN were mixed with normal MDCK cells on collagen gels. The cells were fixed after 24 h incubation with tetracycline and stained with Alexa-Fluor-568-phalloidin (red) and Hoechst (blue). (C) Establishment of MDCK-pTR GFP-RasV12 ZAK-KO cells stably expressing wild-type (WT) or kinase-negative (KN) ZAK. Expression of exogenous ZAK proteins was examined by western blotting using anti-HA antibody. (D) Representative XZ images for the Figure 2d. (C and D) Scale bars: 10 μm.
Knockdown of ZAK in the mouse intestinal epithelium using iGT (E) ZAK-knockdown efficiency of mouse embryonic fibroblasts (MEFs). MEFs were transfected with Control-siRNA (siCtrl), ZAK-siRNA#1 (siZAK#1) or ZAK-siRNA#2 (siZAK#2). After 48 h, the transfected MEFs were subjected to qPCR. Data are mean ± SD from two independent experiments. (F) Immunofluorescence images of ZAK in the epithelium of the small intestine after iGT. The tissue samples were stained with anti-ZAK (magenta) antibody and Hoechst (cyan). Scale bars: 20 μm.
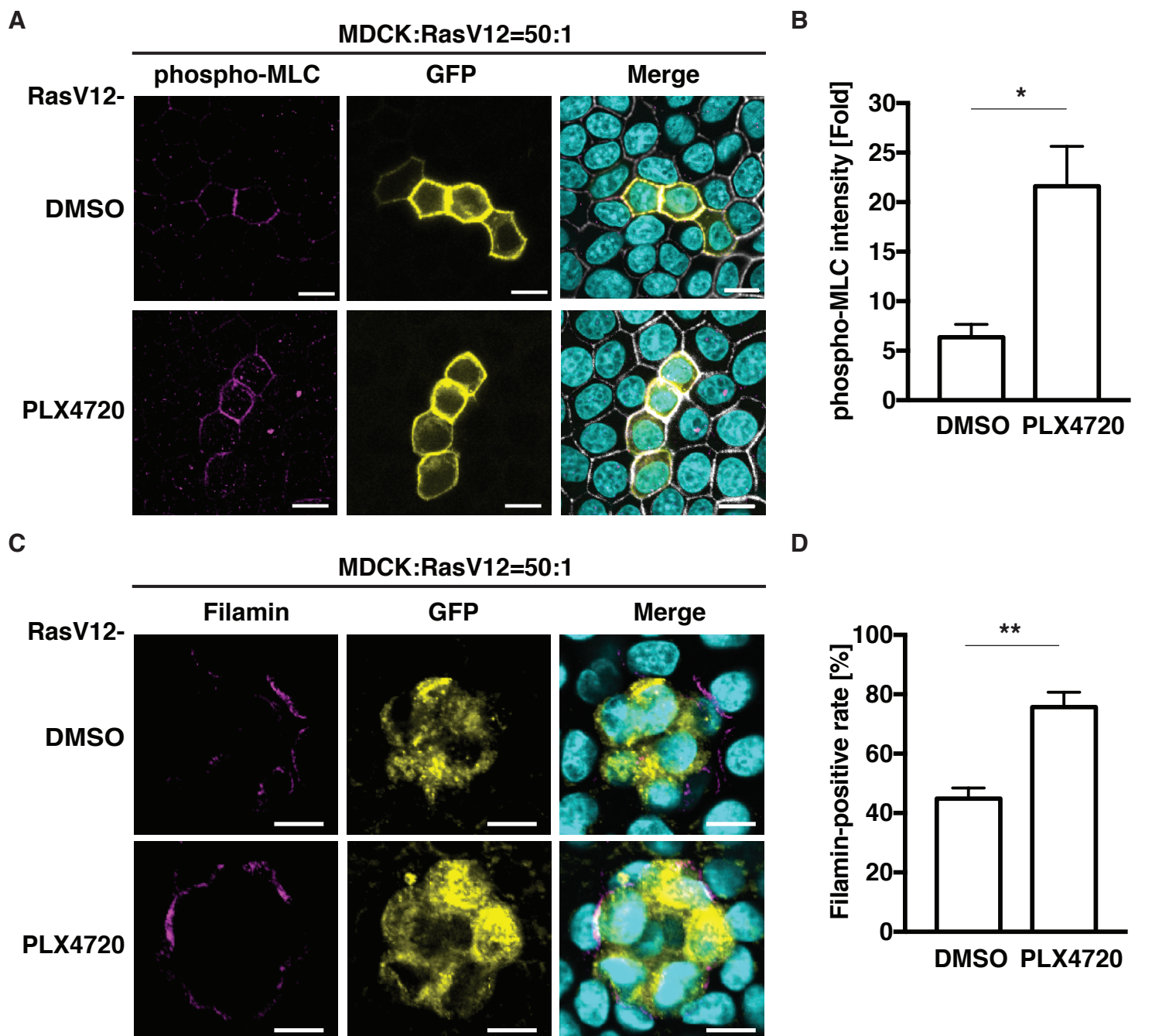
Figure S3. Supplementary figures for Figure 3

(A and B) PLX4720 promotes phosphorylation of light chain of Myosin-II (phospho-MLC) in RasV12 cells surrounded by normal cells. MDCK-pTR GFP-RasV12 cells were mixed with normal MDCK cells on collagen gels. The cells were fixed after 16 h incubation with PLX4720 (1 μM) and tetracycline, and stained with anti-phospho-MLC antibody (magenta), Alexa-Fluor-647-phalloidin (gray) and Hoechst (cyan). For phospho-MLC quantification, the fluorescence intensity at the boundary between respective RasV12 cells and normal cells were expressed as fold change relative to the average fluorescence intesity between the surrounding normal cells. n $\geqq$ 100 cells for each experimental condition. Data are mean ± SD from three independent experiments. *P < 0.05 (Student's t-tests). (C and D) PLX treatment promotes accumulation of Filamin in the neighboring normal cells. MDCK-pTR GFP-RasV12 cells were mixed with normal MDCK cells on collagen gels. The cells were fixed by methanol after 16 h incubation with PLX4720 (1 μM) and tetracycline, and stained with anti-Filamin antibody (magenta) and Hoechst (cyan). The positive rate of Filamin accumulation in surrounding normal cells was quantified. n $\geqq$ 100 cells for each experimental condition. Data are mean ± SD from three independent experiments. **P < 0.01 (Student's t-tests).
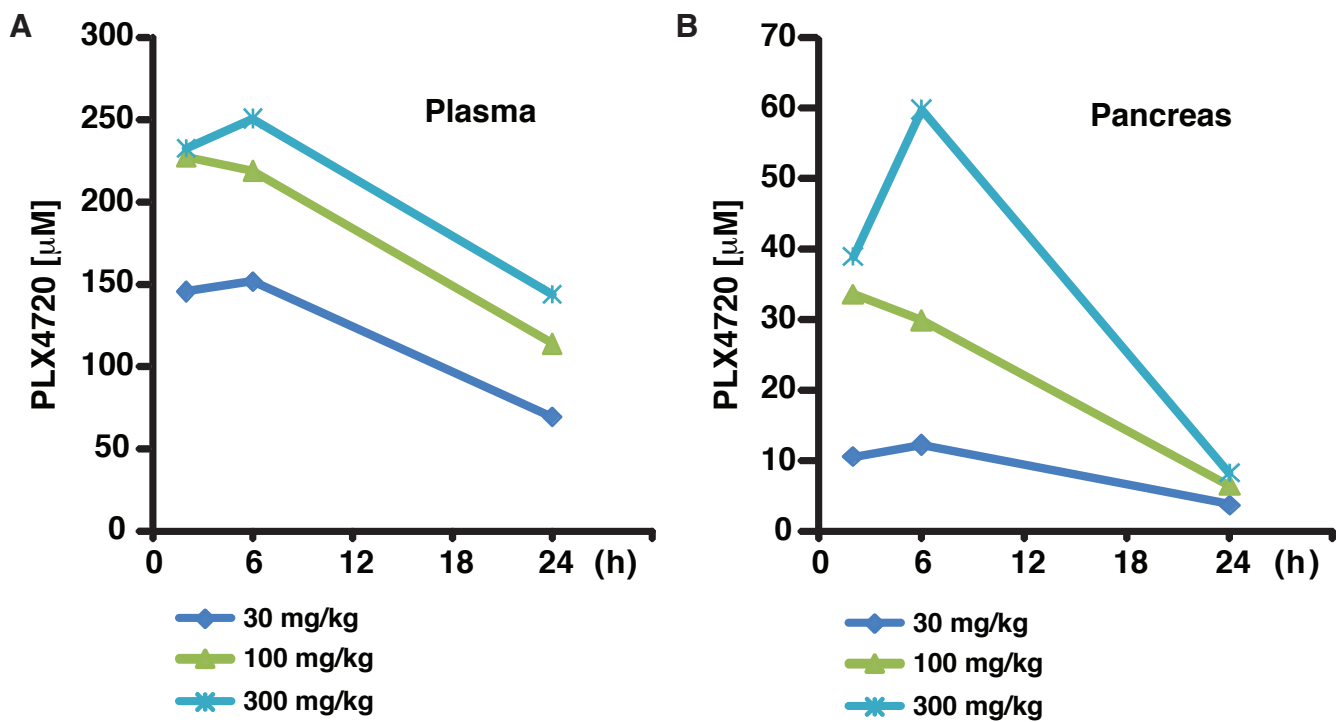
Figure S4. Confirmation of PLX4720-remaining levels, related to Figure 4 (A and B) The remaining PLX4720 in Plasma and Pancreas. The indicated amount of PLX4720 was administered. At the indicated time points after administration, the blood and pancreas were collected. Then, the remaining amounts of PLX4720 in these collected samples were analyzed by mass spectrometry.

	ZAK		BRAFwt		BRAF V600E		ABL1	
	Observed (nM)	Range (nM)	Observed (nM)	Range (nM)	Observed (nM)	Range (nM)	Observed (nM)	Range (nM)
PLX4720	9.47[18], 41[31]	**10-40**	160[32], 330[31], 530[33]	**300-500**	13[32], 32.4[18], 65[33]	**30-70**		
Vemurafenib	4.03[33], 23[18, 20]	**1-20**	100[20]	**100**	31[34], 65[18, 20]	**30-70**		
Dabrafenib	22[20]	**20**	5.2[35, 36]	**5**	0.8[35, 36]	**1**		
Sorafenib	22[37], 6.3[20]	**1-20**	540[20, 37]	**540**	260[16]	**260**	520[16, 37]	**520**

Table S1. The reported IC50 values of individual chemical drugs against the indicated kinases, related to Figure 1

	Name	5' to 3' sequence
Site-directed mutagenesis primer	canis sgZAK1#1_QC_primer_Fw	GGAAAGGACGAAACACCGATTATGAGATGTCGTCTCTGTTTTAGAGCTAGAAATAGC
	canis sgZAK1#1_QC_primer_Rv	GCTATTTCTAGCTCTAAAACAGAGACGACATCTCATAATCGGTGTTTCGTCCTTTCC
Genotyping primer	canis ZAK_geno-primer_exon1_Fw-1	GCCTTGCTTTCCTTTCTCCT
	canis ZAK_geno-primer_exon1_Rv-1	TGTGACCTCTGACTCGGTTG
	CK19-CreERT2 Fw	AATCGCCAGGAATTGACCAATGGGG
	CK19-CreERT2 Rv	CGCCCGTACCCCCAAAGGAAGACAT
	DNMT1-CAG-loxP-STOP-loxP-HRasV12-IRES-eGFP Fw	CACTGTGGAATCTCGGCAGG
	DNMT1-CAG-loxP-STOP-loxP-HRasV12-IRES-eGFP Rv	GCAATATGGTGGAAAATAAC
siRNA sequence	siRNA ZAK #1	GCUGCCUUCCUUUGAGAUUTT
	siRNA ZAK #2	GCUGGACUAAAGUGGAAUAUTT
qPCR primer	mouse ZAKα qPCR_primer_Fw1	acaccaagcatcaacccttc
	mouse ZAKα qPCR_primer_Rv1	gtttctggacagcccatactg
	mouse Actin qPCR_primer_Fw1	aaggccaaccgtgaaaagat
	mouse Actin qPCR_primer_Rv1	gtggtacgaccagaggcatac

Table S2. The sequences of primers and siRNAs used in this study, related to Figure 2, 3 and 4

TRANSPARENT METHODS

(EXPERIMENTAL MODEL AND SUBJECT DETAILS)

Experimental Animals

All animal experiments were conducted under the guidelines by the Animal

Care Committee of Hokkaido University. The animal protocols were reviewed

and approved by the Hokkaido University Animal Care Committee (approval

number 12-0116). We used 6-10 weeks-old C57BL/6 mice for mating.

Cytokeratin19 (CK19)-CreERT2 mice (Means et al., 2008) were crossed with

DNMT1-CAG-loxP-STOP-loxP-HRasV12-IRES-eGFP mice (Kon et al., 2017) to

create CK19-RasV12-GFP mice. Mice heterozygous for each transgene were

used for experiments.

Cell Lines

MDCK and MDCK-pTR GFP-RasV12 cells were cultured as previously

described (Hogan et al., 2009).

METHOD DETAILS

Cell competition-based high-throughput screening for chemical compounds using confocal microscopy

For the confocal microscopy-based primary screening, 5×10^3 MDCK-pTR GFP-RasV12 cells were mixed with 4.5×10^4 MDCK cells and seeded into a collagen-coated 96-well plate. The mixed cells were incubated at 37°C for 24 h until a monolayer was formed. Then, the culture medium was exchanged for new medium containing 10 μg ml^{-1} tetracycline and 10 μM each small chemical compound (Kinase inhibitor library I, SIGMA-ALDRICH), followed by further incubation for 16 h. Finally, cells were washed with PBS, fixed in 4% paraformaldehyde (PFA) /PBS, and stained with Hoechst 33342 and Alexa555-Phalloidin. The images of cells were captured by using a confocal imaging analyzer, IN CELL Analyzer 6000 (GE Healthcare). To evaluate the extrusion levels of GFP-RasV12 cells, the extruded GFP-positive cells from a cell monolayer were analyzed using a 65536-gradient step bright-field, and GFP-positive extruded cells were shown as white spots.

Antibodies and Materials

Chicken anti-GFP (ab13970) and rabbit anti-ZAK (ab65249) antibodies were

purchased from Abcam. Rat anti-E-cadherin (131900) antibody was from Life

Technologies. Anti-Paxillin (sc-5574) antibody was from Santa Cruz

Biotechnology. Rabbit anti-phospho-MLC 2 (Thr18/Ser19; 3674) antibody was

from Cell Signaling Technology. Mouse anti-Filamin (F6682) antibody was from

Sigma-Aldrich. Mouse anti-Actin (MAB1501R) and mouse anti-HA (05-904)

antibodies were from Merck Millipore. Alexa-Fluor-568- and -647-conjugated

secondary antibodies were from ThermoFisher Scientific. Hoechst 33342 (Life

Technologies) was used at a dilution of 1:5,000. For immunofluorescence, the

primary antibodies described above were diluted in PBS containing 1% BSA at

1:100, except anti-Paxillin antibody at 1:50. All secondary antibodies were used

at 1:200. Alexa-Fluor-568- and -647-conjugated Phalloidin (Life Technologies)

were used at 1.0 U ml^{-1}. PLX4720, Vemurafenib, Dabrafenib, and Sorafenib

were purchased by Chemscene LLC. DMSO (Sigma-Aldrich) was added as a

control.

Cell Culture

MDCK and MDCK-pTR GFP-RasV12 cells were cultured as previously

described (Hogan et al., 2009). To induce the expression of GFP-RasV12, the

tetracycline-inducible MDCK-pTR GFP-RasV12 cell lines were treated with 2 μg

ml^{-1} tetracycline (Sigma-Aldrich). For the inhibitor treatment, the indicated

inhibitors were added together with tetracycline, and cells were then cultured for

16 h or 24 h. For immunofluorescence, cells were seeded onto Type-I collagen-

mounted coverslips as described below in the section of immunofluorescence.

CRISPR/Cas9-mediated generation of ZAK-knockout cells

Guide sequences of ZAK single-guide RNA (sgRNA) targeting canis ZAK were

designed on exons 1 as described previously (Hsu et al., 2013). ZAK sgRNA

sequences (ZAK sgRNA, 5'-ATTATGAGATGTCGTCTCT-3') were introduced

into the pCDH-QC-sgRNA control (sgControl) vector (Maruyama et al., 2015)

using primers listed in Table S2. First, MDCK cells were infected with lentivirus

carrying pCW-Cas9 as described (Maruyama et al., 2015) and were cultured in

the 500 ng ml^{-1} puromycin-containing medium. The tetracycline-inducible

MDCK-Cas9 cells were transfected with the pCDH-QC-ZAK sgRNA (sgZAK) by

nucleofection, followed by selection in medium containing 200 μg ml^{-1}

hygromycin. The antibiotics-selected crude Cas9-sgControl or sgZAK MDCK

cells were lysed with quick extraction buffer (Epicentre), and the lysates were

subjected to PCR. The PCR amplicons were digested with Surveyor enzyme

(Integrated DNA Technologies). The crude cells were subjected to limiting dilution, and indels on the ZAK first exon in isolated monoclone were analyzed by direct sequencing using primers listed in Table S2. ZAK-KO cell lines which possess 2 base-homozygous depletion (KO1) or 17 base-homozygous insertion (KO2) were obtained. To generate ZAK-deleted cells carrying tetracycline-inducible GFP-RasV12, pPB-TRE3 GFP-RasV12 was introduced into the ZAK-deleted cells by nucleofection and antibiotic selection (Blasticidin, 5 μg ml^{-1}). In addition to the ZAK-KO MDCK-pTRE3G GFP-RasV12 cells, we generated ZAK-WT MDCK-pTRE3G GFP-RasV12 cells as a control cell line. To constitutively express HA-ZAK-WT or HA-ZAK-KN, MDCK-pTRE3G GFP-RasV12 ZAK-KO1 cells were transfected with PB-HA-ZAKα-WT or -KN and subjected to antibiotics selection (G418, 800 μg ml^{-1}).

Immunofluorescence

For immunohistochemical examinations of the small intestine and pancreas, the mice were perfused with 1% PFA (Sigma-Aldrich), and the isolated tissues were fixed with 4% PFA in PBS for 24 h and embedded in FSC 22 Clear Frozen Section Compound (Leica Biosystems). Then, 10-μm-thick frozen sections were cut on a cryostat. The sections were blocked with Block-Ace (DS Pharma

Biomedical) and 0.1% Triton X-100 in PBS. Primary or secondary antibodies were incubated for 2 h or 1 h respectively at ambient temperature. All primary antibodies were used at 1:1,000, and all secondary antibodies were at 1:500 except for ZAK antibody (1:100). For immunofluorescence of cultured cells, MDCK-pTR GFP-RasV12 cells were mixed with MDCK cells at a ratio of 1:50 and cultured on the collagen matrix as previously described (Hogan et al., 2009). The mixture of cells was incubated for 8-12 h until they formed a monolayer, followed by tetracycline treatment for 24 h. Cells were fixed with 4% PFA in PBS and permeabilized with 0.5% Triton X-100 in PBS, except for Filamin immunofluorescence for which cells were fixed in methanol at -20°C for 2.5 min as shown in Figures 3E and S3C, followed by blocking with 1% BSA in PBS. Alexa-Fluor-568- or -647-conjugated Phalloidin was incubated for 1 h at ambient temperature. Immunofluorescence images of mouse tissues and cultured cells were acquired using the Olympus FV1000 system and Olympus FV10-ASW software. Paxillin, ppMLC and Filamin-stained images were quantified with the ImageJ software.

***In vivo* mouse model and PLX treatment**

All animal experiments were conducted under the guidelines by the Animal

Care Committee of Hokkaido University. The animal protocols were reviewed

and approved by the Hokkaido University Animal Care Committee (approval

number 12-0116). We used 6-10 week-old C57BL/6 mice for mating.

Cytokeratin19 (CK19)-CreERT2 mice (Means et al., 2008) were crossed with

DNMT1-CAG-loxP-STOP-loxP-HRasV12-IRES-eGFP mice (Kon et al., 2017) to

create CK19-RasV12-GFP mice. Male and female mice heterozygous for each

transgene were used for experiments. For PCR genotyping of mice, the

sequence information of the used primers is shown in Table S2. Mice were age-

matched and given a single intraperitoneal injection of 0.5 mg of tamoxifen

(TAM) in corn oil (Sigma-Aldrich) per 20 g of body weight for the induction of

RasV12 expression, and then sacrificed at Day 6 or Day 30 after Cre activation.

To examine the effect of PLX4720, the mice were pretreated with an oral

beverage of 300 mg l^{-1} PLX4720 at the post 1 day after TAM injection.

In vivo electroporation

The iGT (intestine-specific gene transfer) using HVJ-E (haemagglutinating virus

of Japan envelope) was modified and performed as follows (Imajo et al., 2015;

Kon et al., 2017). Briefly, 3-5 cm regions of the small intestine drawn out from

the peritoneal cavity were tied with nylon string. 300 μl of the mucus removing

solution (20 mM DTT and 0.05% Tween-20 in PBS) was injected into the

intestinal lumen for 15 min, removed and incubated with the same solution for

10 min. After washing with PBS three times by pipetting, 300 μl of Opti-MEM

(Thermo Fisher Scientific) containing Cy3-labelled siRNA was injected, and the

tied part of intestine was sandwiched with electro-nodes (NEPAGENE;

CUY650P5) for electroporation (condition: Voltage; 40 V, Pulse; 30 ms, Interval;

50 ms, 3 times, reduction; 10%). The sequences of ZAK-siRNA are listed in

Table S2. 0.5 mg of TAM was injected into the peritoneal cavity when the wound

was sutured. The mice were euthanized for analysis after 5 days of iGT.

Reverse Transcription and Quantitative PCR Analysis

Total RNA was extracted from isolated cell samples using Sepazol (Nacalai

Tesque) and chloroform, precipitated with 2-propanol and washed with 75%

(vol/vol) ethanol. RNA samples were incubated with DNase I (Invitrogen) to

remove contaminating genomic DNA and then reverse-transcribed into cDNA

(Superscript III reverse transcriptase, VIRO cDNA Synthesis Kit; Invitrogen).

Quantitative PCR analysis was performed using LightCycler 480 II (Roche) with

FastStart Essential DNA Probes Master (Roche). Primer sequences are shown

in the Table S2.

QUANTIFICATION AND STATISTICAL ANALYSIS

Two-tailed Student's *t*-tests or Chi-squared tests were used to determine *P*-

values for statistical analyses. For quantification of the apical extrusion

frequency, more than 100 transformed cells are subject to the apical extrusion

analysis in each sample. For quantification of the immunofluorescence intensity,

at least 30 transformed cells were analyzed using the ImageJ software for each

experimental condition.